International Journal of Engineering & Technology, 7 (4.14) (2018) 454-457

International Journal of Engineering & Technology

Website: www.sciencepubco.com/index.php/IJET

Research paper

Effect of Deposition Time of Mn on Photoelectrochemical Properties of Mn/TiO_2 Nanotubes

Asmaa Kadim Ayal[1]*, Ahlam Mohammed Farhan[1], Ying-Chin Lim[2]

[1] *Department of Chemistry, College of Science for Women, University of Baghdad, Baghdad, Iraq*
[2] *School of Chemistry and Environment, Faculty of Applied Sciences, Universiti Teknologi MARA, 40450 Shah Alam, Selangor, Malaysia*
** Corresponding author E-mail: asmaakadem@yahoo.com*

Abstract

Coupling of TiO_2 nanotube arrays (NTAs) with narrow band gap materials has been a promising strategy to extend the absorption of TiO_2 into visible light region. In this work, the fabrication of manganese doped TiO_2 nanotube arrays (Mn/TiO_2 NTAs) was carried out by an electrodeposition method. The deposition time of Mn onto TiO_2 NTAs which was varied in the range of 1-5 minutes was found to play an important role in controlling the formation and distribution of Mn nanoparticles onto TiO_2 NTAs. The films were characterized by field emission scanning electron microscopy (FESEM), X-ray diffractometry (XRD), energy dispersive X-ray spectroscopy (EDX) and UV–vis diffuse reflectance spectroscopy to determine their morphology, crystalline structure, and optical properties of the samples. The results from FESEM showed that Mn nanoparticles were found to grow larger and cause blockage to the mouth of the nanotubes with prolongs deposition time. On the other hand, Mn/TiO_2 NTAs synthesized with shorter deposition time exhibits significant enhancements in the optical absorption and photocurrent density. In particular, the Mn/TiO_2 NTAs produced at 1minute deposition time exhibited the highest photocurrent density compared to the others. The uniform distribution and quantity of the Mn could be the reason for this performance, therefore, more light was absorbed and generating more electron-hole pairs then giving the highest photocurrent.

Keywords: *TiO_2 nanotube; Mn/TiO_2 nanotube; deposition time; electrochemical deposition; photoelectrochemical.*

1. Introduction

TiO_2 is a semiconductor material with low toxicity, good chemical stability, environmentally friendly nature, low cost, and naturally abundance [1-3]. During the last decade, it has been intensively studied for many applications in the energy and environment field, such as supercapacitors, photelectrochemical cells, gas sensors, pollutant cleansers, and photocatalysts [4-5].

The morphology of materials has a considerable effect on their chemical and photoelectrochemical properties [6]. TiO_2 nanotube arrays (NTAs) synthesized via anodization technique, with high surface areas and well-ordered structures is of improved or new character in comparison to other different morphologies (nanorod, nanoparticles, nanobelts). For instance, the TiO_2 NTAs exhibited considerably superior light harvesting efficiencies and greater charge collection efficiencies than TiO_2 nanoparticles [7]. Because of the back contacted TiO_2 NTAs layers on the Ti substrate, thus it can be used as supercapacitors [4, 8-9]. TiO_2 NTAs has been used in a broader area of applications, for example, as photocatalyst [10], in dye-sensitized solar cell [11], and photoelectrochemical cells [12]. In order to improve the photoelectrochemical properties of TiO_2 NTAs, many research efforts on modification of TiO_2 NTAs have been carried out. Our previous studies on the modification of TiO_2 NTAs included the deposition of CdS [13] and CdSe [14] onto TiO_2 NTAs. Deposition of metal ions onto TiO_2 NTAs is one of the effective methodologies to improve the photoelectrochemical properties of TiO_2 NTAs as the absorption into visible light region by TiO_2 could be extended via lowering band gap energy effect of the metal dopant as Nb, Zr, Bi, and V [15-17]. Doping is necessary to modify the intrinsic property of semiconducting nanocrystals like Mn. One of the promising metal dopant is Mn. Manganese is abundant in the earth and therefore, low cost, and has newly attracted much interest as a visible light sensitizer. To the best of our knowledge, there are little reports on the photoelectrochemical properties of Mn deposited into TiO_2 NTAs. In this study, Mn was deposited into TiO_2 NTAs via a two-step electrodeposition anodization method and their crystal structures, morphologies, and photoelectrochemical properties were examined. Moreover, as a comparison, the TiO_2 NTAs were also synthesized using the same procedure and were characterized accordingly.

2. Experimental

2.1. Preparation of TiO_2 NTA and Mn/TiO_2 NTAs

Anodization technique was executed by a program controlled DC source. The anodization set-up consists of a two-electrode electrochemical configuration with a Ti foil acts as the anodic electrode and a high-density graphite as the cathodic electrode. The electrolyte used in this procedure was 95% volume ratio of ethylene glycol solution containing 0.5 wt% NH_4F and 5% volume ratio of water. The anodization process was conducted at 40 V for 1 hour. After the anodization, the sample was rinsed with DI water, air-dried, and subjected to further annealing at 500 ˚C for 2 h with 2^oC/ min rate of heating. A heat treatment is necessary to induce crystallinity in the TiO_2 NTAs. To deposit Mn into TiO_2 NTAs, electrodeposition technique was carried out with a two-electrode electrochemical cell containing 5mM of $Mn(NO_3)_2$. H_2O electrolyte. The prepared TiO_2 NTAs was placed at the cathode and the

graphite acts as the anode. Electrodeposition of Mn was executed at 4V for various times of deposition (1, 2, 3, 4, and 5) min. Then, DI water was used to rinse the sample and subsequently they were dried in air and subjected for further characterization.

2.2. Characterization methods of TiO_2 NTAs and Mn/ TiO_2 NTAs

The morphological of TiO_2 NTAs and Mn/ TiO_2 NTAs were studied via Field Emission Scanning Electron Microscope (FESEM, JSM-7600F, JOEL, Japan) while Energy Dispersive X-Ray (EDX) spectrophotometer coupled with FESEM was used to analyze the elemental composition of the sample. The X-Ray Diffractometer (Panalytical X, Pert Pro MPD with CuKa radiation, k = 1.5406 A°) working at 40 kV and 40 mA was used to determine the crystal structures and crystallinity of the samples. UV–Vis diffuse reflectance spectrophotometer (Cary 300, USA) was used to measure the optical absorption of the samples. Finally, a three electrode photoelectrochemical (PEC) cell connected to potentiostat was used to evaluate the photoelectrochemical properties of the sample. In the PEC cell, the Mn/TiO_2 NTAs as the working electrode, a Pt wire as the counter electrode, and an Ag/AgCl as the reference electrode, was used to evaluate photocurrent response of the prepared samples. The measurements of current were executed in 0.01 M Na_2S under intermittent illumination from a halogen lamp (300 W) where both the photocurrent and dark current were recorded in a single experiment. The photocurrent was recorded by (Autolab PGSTAT204/FRA32 M module) with a scan rate of 20 mV s^{-1}.

3. Results and discussion

The FESEM images of blank and modified TiO_2 NTAs are displayed in Fig.1. Upon anodization, well-ordered TiO_2 NTAs were formed and was used as the substrate for subsequent deposition of Mn. The diameter of TiO_2 NTAs is about 60–90 nm as shown in Fig. 1a. Fig. (1b-1f) displays that the morphology of Mn nanoparticles different greatly with the alteration of deposition time. Fig 1b displays the uniform distribution of spherical liked Mn nanoparticles on the TiO_2 NTAs. As expected, with increasing deposition time of Mn onto TiO_2, the particles size of Mn was increased and eventually covered the tubes opening as shown in Fig (1c- 1f). The wall of nanotubes was seen to be thickening as a result of the deposition of Mn. At 4 mins, the opening of the nanotubes' mouth still can be observed and the blockage of the mouth is quite severe at 5 mins deposition time.

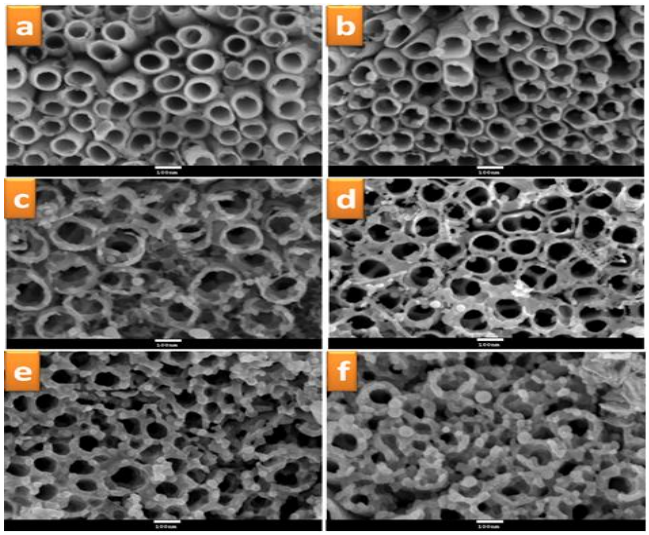

Fig. 1: Top view FESEM images of (a) TiO_2 NTAs and Mn deposited into TiO_2 NTAs at different deposition time: (b) 1, (c) 2, (d) 3, (e) 4 and (f) 5 mins

XRD analysis of TiO_2 NTAs and Mn/TiO_2 NTAs samples were conducted and the results are displayed in Fig.2. TiO_2 NTAs shows sharp anatase peaks at 2θ = 25.7°, 37.5°, 48.5°, 54.0° and 55.0°, respectively (JCPDS: 21-1272). The intense and sharp peaks indicate that the sample is highly crystalline. Moreover, there were peaks which attributed to the titanium phase at 2θ = 35.45°, 38.8°, 40.5°, and 53.4°, respectively. Furthermore, a small peak at 2θ = 31.8° was attributed to Mn phase (JCPDS No. 00-001-1234). From this result, XRD analysis confirmed the presence of Mn into TiO_2 NTAs.

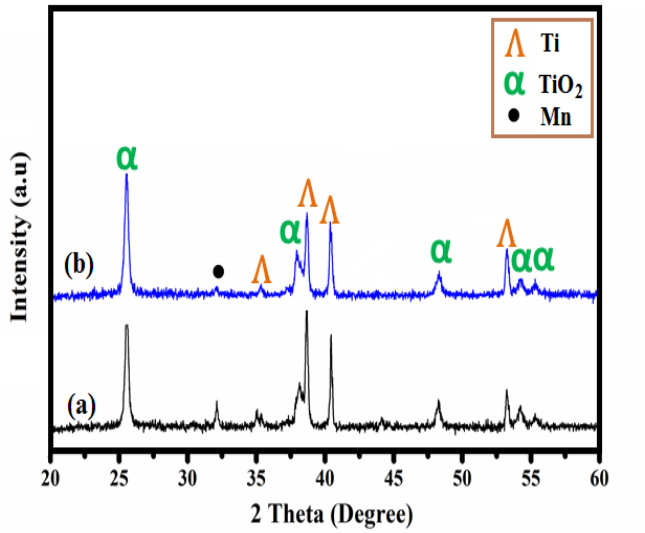

Fig. 2: XRD patterns of: (a) TiO_2 NTAs, (b) Mn/TiO_2 prepared at 1 min deposition time.

The elemental composition of the Mn decorated with TiO_2 NTAs was additionally measured via EDX as presented in Fig. 3. The featured characteristic peaks in the spectrum of EDX are associated with Mn, Ti, and O, confirming the deposition of Mn onto TiO_2 NTAs was a successful one. No other impurities were detected.

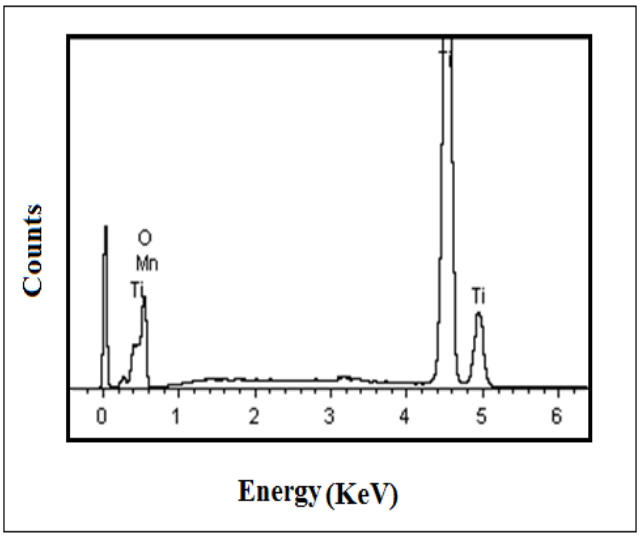

Fig. 3: EDX spectra of Mn/TiO_2 NTAs prepared at 1 min deposition time

Fig. 4 shows the UV–DRS absorbance spectra of TiO_2 NTAs and Mn/TiO_2 NTAs in the range of 350 to 700 nm. In this work, the absorption edge of TiO_2 NTAs was detected less than 400 nm ascribed to the fundamental inter-band transition absorption of TiO_2 NTAs. The low absorption of pure TiO_2 NTAs in the visible area can be attributed to the presence of cracks or pores and oxygen vacancies in TiO_2 NTAs is responsible for the light scattering [18-19]. It is observed that all Mn/TiO_2 NTAs samples display a high absorption in the wavelengths between 400 to 700 nm, com-

pared to the bare TiO_2 NTAs, which confirmed the ability of Mn/TiO_2 NTAs samples to absorb the visible light. The absorption edge clearly has been shifted to the visible area (red-shift). This possibly attributed to the incorporation of Mn onto TiO_2 NTAs has well narrowed down band gap of Mn/TiO_2 NTAs as shown in Table 1. The optical bandgap was calculated by using the equation: Eg (eV) = 1240/(wavelength in nm).

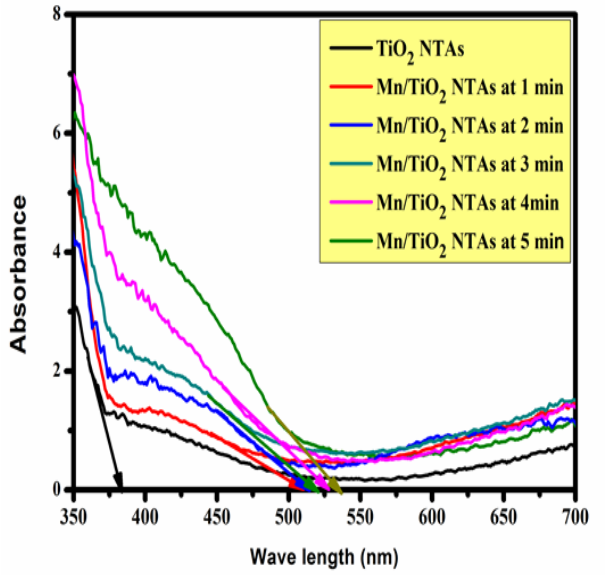

Fig. 4: UV–Vis absorption curves: TiO_2 NTAs and Mn/TiO_2 NTAs prepared at various deposition times

Table 1: Absorption edge and band gap energy values of Mn/TiO_2 NTAs prepared at different deposition time

Thin film	Absorption edge (nm)	Observed band gap values (eV)
TiO_2 NTAs	382	3.24
Mn/TiO_2 NTAs at 1 min deposition time	507	2.44
Mn/TiO_2 NTAs at 2 min deposition time	511	2.42
Mn/TiO_2 NTAs at 3 min deposition time	521	2.38
Mn/TiO_2 NTAs at 4 min deposition time	529	2.34
Mn/TiO_2 NTAs at 5 min deposition time	536	2.31

Fig. 5 shows the photoelectrochemical response of bare TiO_2 NTAs and Mn/TiO_2 NTAs photoelectrodes using a three-electrode electrochemical cell with a Pt wire electrode as a counter and saturated Ag/AgCl electrode as reference, under halogen light irradiation. The photocurrent measurements were carried out in a 0.1 M Na_2S as electrolyte. As a consequence, TiO_2 NTAs has absorbed a few parts of the photons to the generation of a photocurrent [20] [21]. Thus, it is substantial to take the photocurrent/voltage feature for further realization of the photoelectrochemical properties of Mn/TiO_2 NTAs. The photocurrent density of Mn/TiO_2 NTAs photoelectrode is higher than that of a bare TiO_2 NTAs photoelectrode at all bias potential because of a decrease recombination of photogenerated holes and electrons after Mn has been deposited into TiO_2 NTAs. Hence Mn doping may cause the electrons to get trapped and screen them from charge recombination with holes, leading to the improvement of charge collection efficiency. The highest photocurrent generated by Mn deposited into TiO_2 NTAs at 1 min deposition time due to enhanced optical absorption and improved in the crystallinity caused by Mn deposited into TiO_2 NTAs [20]. The results confirm that the Mn deposited into TiO_2 NTAs are sensitive to the visible light and can produce a sustainable regular photocurrent under halogen (visible) light irradiation.

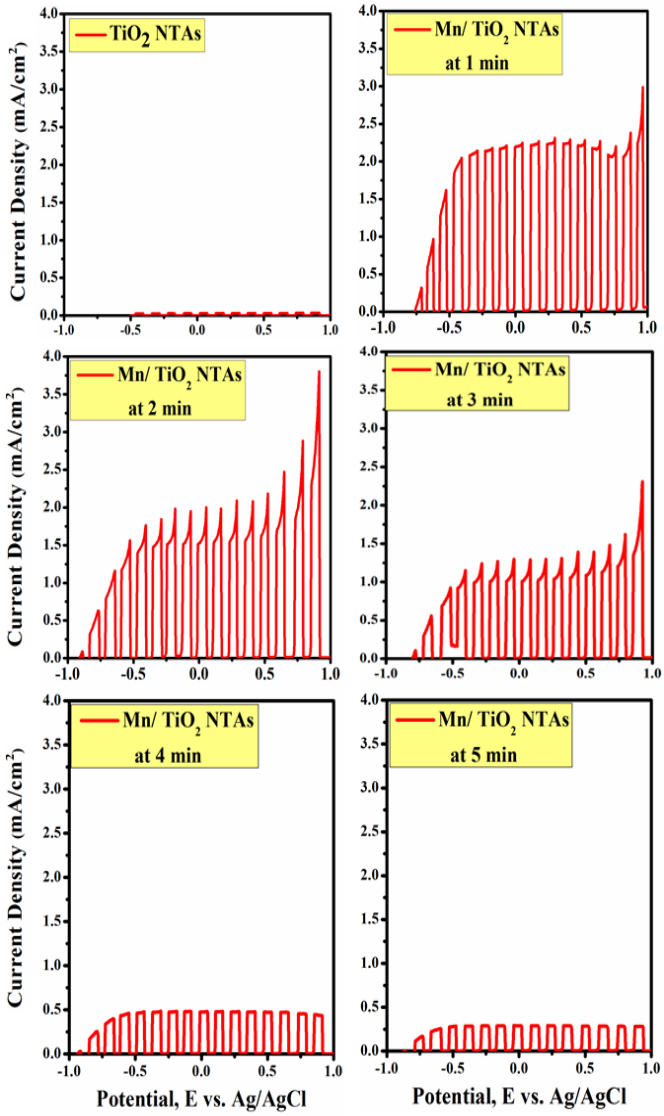

Fig. 5: Photocurrent density, I–V curve in 0.01 M Na_2S: TiO_2 NTAs and Mn/TiO_2 NTAs prepared at various deposition time

4. Conclusion

In this paper, TiO_2 NTAs were successfully doped with manganese using an electrodeposition method. Depositing manganese extended the absorption of TiO_2 NTAs films into the visible light region. Under visible light (halogen lamp) irradiation, the Mn/TiO_2 NTAs films displayed higher photocurrent response than the undoped TiO_2 NTAs films. These amended properties can be imputed to the increased absorption of visible light, the improved surface defects and the photogenerated electrons/hole separation generated by Mn depositing into TiO_2 NTAs.

Acknowledgement

The authors thank Chemistry and Physics Departments, Faculty of Science, and Microscopy Unit, Institute of Bioscience, Universiti Putra Malaysia.

References

[1] H. Wu, D. Li, X. Zhu, C. Yang, D. Liu, X. Chen, Y. Song, and L. Lu, "High-performance and renewable supercapacitors based on TiO_2 nanotube array electrodes treated by an electrochemical doping approach," Electrochim. Acta, vol. 116, (2014), pp. 129–136.

[2] S. Liu, Z. Wang, C. Yu, H. Bin Wu, G. Wang, Q. Dong, J. Qiu, A. Eychmüller, X. Wen, and D. Lou, "A Flexible TiO_2 (B) -Based Battery Electrode with Superior Power Rate and Ultralong Cycle Life," Adv. Mater., vol. 2, (2013), pp. 1–6.

[3] P. Roy, S. Berger, and P. Schmuki, "TiO_2 nanotubes: Synthesis and applications," Angew. Chemie - Int. Ed., vol. 50, no. 13, (2011), pp. 2904–2939.

[4] V. A. Online, H. Li, Z. Chen, C. K. Tsang, Z. Li, X. Ran, C. Lee, B. Nie, L. Zheng, T. Hung, J. Lu, B. Pan, and Y. Y. Li, "Electrochemical doping of anatase TiO_2 in organic electrolytes for high-performance supercapacitors and photocatalysts †," J. Mater. Chem. A, vol. 2, (2014), pp. 229–236.

[5] M. Z. Lin, H. Chen, W. F. Chen, A. Nakaruk, P. Koshy, and C. C. Sorrell, "Effect of single-cation doping and codoping with Mn and Fe on the photocatalytic performance of TiO_2 thin films," Int. J. Hydrogen Energy, (2014), pp. 1–12.

[6] Y. Yang, G. Ruan, C. Xiang, G. Wang, and J. M. Tour, "Flexible Three-Dimensional Nanoporous Metal-Based Energy Devices," Am. Chem. Soc., vol. 136, (2014), pp. 6187–6190.

[7] K. Zhu, N. R. Neale, A. Miedaner, and A. J. Frank, "Enhanced charge-collection efficiencies and light scattering in dye-sensitized solar cells using oriented TiO_2 nanotubes arrays," Nano Lett., vol. 7, no. 1, (2007), pp. 69–74.

[8] M. Salari, S. H. Aboutalebi, K. Konstantinov, and H. K. Liu,"A highly ordered titania nanotube array as a supercapacitor electrode," Phys. Chem. Chem. Phys., vol. 13, (2011), pp. 5038–5041.

[9] X. Xia, J. Luo, Z. Zeng, C. Guan, Y. Zhang, J. Tu, and H. Zhang, "Integrated photoelectrochemical energy storage : solar hydrogen generation and supercapacitor," Sci. Rep., vol. 2, (2012), pp. 1–6.

[10] H. Li, J. Wang, M. Liu, H. Wang, P. Su, J. Wu, and J. Li, "A nanoporous oxide interlayer makes a better Pt catalyst on a metallic substrate: Nanoflowers on a nanotube bed," Nano Res., vol. 1, (2014), pp. 1–11.

[11] H. Wang, H. Li, J. Wang, J. Wu, D. Li, M. Liu, and P. Su, "Nitrogen-doped TiO_2 nanoparticles better TiO_2 nanotube array photoanodes for dye sensitized solar cells," Electrochim. Acta, vol. 137, (2014), pp. 744–750.

[12] A. Kadim, Z. Zainal, H. Ngee, Z. Abidin, Y. Lim, S. Chang, and A. Mebdir, "Fabrication of CdSe nanoparticles sensitized TiO_2 nanotube arrays via pulse electrodeposition for photoelectrochemical application," Mater. Res. Bull., vol. 106, no. December 2017, (2018), pp. 257–262.

[13] A. K. Ayal, "Enhanced Photocurrent of Titania Nanotube Photoelectrode Decorated with CdS Nanoparticles," Baghdad Sci. J., vol. 15, no. 1, (2018), pp. 57–62.

[14] A. K. Ayal, Z. Zainal, H.-N. Lim, Z. A. Talib, Y.-C. Lim, S.-K. Chang, and A. M. Holi, "Photocurrent enhancement of heat treated CdSe-sensitized titania nanotube photoelectrode," Opt. Quantum Electron., vol. 49, no. 4, (2017), pp.1-11.

[15] H. Jha, R. Hahn, and P. Schmuki, "Ultrafast oxide nanotube formation on TiNb, TiZr and TiTa alloys by rapid breakdown anodization," Electrochim. Acta, vol. 55, no. 28, (2010), pp. 8883–8887.

[16] J. Yang, X. Wang, X. Yang, J. Li, X. Zhang, and J. Zhao, "Energy storage ability and anti-corrosion properties of Bi-doped TiO_2 nanotube arrays," Electrochim. Acta, vol. 169, (2015), pp. 227–232.

[17] Y. Yang, D. Kim, M. Yang, and P. Schmuki, "Vertically aligned mixed V_2O_5 – TiO_2 nanotube arrays for supercapacitor applications," Chem. Commun., vol. 47, (2011), pp. 7746–7748.

[18] H. Wang, Y. Yang, and J. Wei, "Effective photocatalytic properties of N doped Titanium dioxide nanotube arrays prepared by anodization," Reac Kinet Mech Cat, vol. 106, (2012), pp. 341–353.

[19] S. Zhang, F. Peng, H. Wang, H. Yu, S. Zhang, J. Yang, and H. Zhao, "Electrodeposition preparation of Ag loaded N-doped TiO_2 nanotube arrays with enhanced visible light photocatalytic performance," Catal. Commun., vol. 12, no. 8, (2011), pp. 689–693.

[20] J. Li, N. Lu, X. Quan, S. Chen, and H. Zhao, "Facile Method for Fabricating Boron-Doped TiO_2 Nanotube Array with Enhanced Photoelectrocatalytic Properties," Ind. Eng. Chem. Res, vol. 47, (2008), pp. 3804–3808.

[21] G. Yan, M. Zhang, J. Hou, and J. Yang, "Photoelectrochemical and photocatalytic properties of N + S co-doped TiO_2 nanotube array films under visible light irradiation," Mater. Chem. Phys., vol. 129, no. 1–2, (2011), pp. 553–557.